

## Short communication

One step simultaneous synthesis of modified-CVD-made  
 $V_2O_5/TiO_2$  nanocomposite particlesMin Young Song<sup>a,b</sup>, Sungmin Chin<sup>a</sup>, Jongsoo Jurng<sup>a,\*</sup>, Young-Kwon Park<sup>b,c,\*\*</sup><sup>a</sup> Environmental Sensor System Research Center, Korea Institute of Science and Technology (KIST),  
39-1, Hawolgok, Seongbuk, Seoul 136-791, Republic of Korea<sup>b</sup> Graduate School of Energy and Environmental System Engineering, University of Seoul, Seoul 130-743, Republic of Korea<sup>c</sup> School of Environmental Engineering, University of Seoul, Seoul 130-743, Republic of Korea

Received 4 October 2011; received in revised form 7 November 2011; accepted 8 November 2011

Available online 18 November 2011

## Abstract

A one step simultaneous synthesis of  $V_2O_5/TiO_2$  nanocomposite particles was carried out using a modified-chemical vapor deposition (CVD) process employing two metal-organic precursors. The flow rate of the vanadium precursor was varied from 0 to 3 L/min with the flow rate of the TTIP precursor kept constant. The pure  $TiO_2$  and prepared  $V_2O_5/TiO_2$  nanocomposite particles were examined by BET, XRD, XPS, TEM and SEM-EDS. The results showed that both the vanadium concentration and particle size increased with increasing flow rate of the vanadium precursor, whereas the specific surface area decreased. XPS confirmed that the nanocomposite particles consisted of Ti, V and O. The  $V_2O_5/TiO_2$  nanocomposite particles had a mean size of 20–40 nm. TEM showed that the flow rate had a significant effect on the particle size. The  $V_2O_5/TiO_2$  nanocomposite particles are expected to have a wide range of applications in many fields, such as catalysts, photoelectron materials and sensors. © 2011 Elsevier Ltd and Techna Group S.r.l. All rights reserved.

**Keywords:** One step simultaneous synthesis; Modified-chemical vapor deposition;  $V_2O_5/TiO_2$  nanocomposite particles

## 1. Introduction

The synthesis of  $V_2O_5/TiO_2$  nanocomposite particles has attracted considerable attention because of their wide range of potential applications, such as catalysts, photoelectron materials and sensors [1–3]. Spreading vanadium over the  $TiO_2$  support leads to a modification of the chemical–physical properties of the former as well as to enhanced catalytic properties [4–6]. The structural characteristics, activity and selectivity of the  $V_2O_5/TiO_2$  systems depend mainly on the method and preparation conditions, such as the crystallographic  $TiO_2$  structures employed, vanadium loading and calcination temperature [7]. Among the range of methods used to prepare nanocomposite particles, such as liquid phase deposition, wet impregnation, vacuum evaporation, sol–gel process and

chemical vapor deposition (CVD) [8–12], CVD can be used to prepare a range of materials and produce a large amount of nanoparticles. The characteristics of the particles finally formed are affected by the preparation parameters, such as the flow rate of the carrier gas and the decomposition temperature of the precursors [13]. Many studies have evaluated the synthesis materials in a CVD process [14–16], but few have examined the simultaneous synthesis of composite materials.

This study employed two precursors for a one step synthesis of nanocomposite particles by CVD as a simple and modified method that was superior to the traditional CVD process. In this study,  $V_2O_5/TiO_2$  nanocomposite particles were synthesized in a one step using a modified-CVD process employing two metal-organic precursors. The effect of the vanadium concentration on the structural characteristics of the  $V_2O_5/TiO_2$  nanocomposite particles was also examined by adjusting the flow rate of the vanadium precursor.

## 2. Experimental

The  $V_2O_5/TiO_2$  nanocomposite particles were synthesized using a modified-CVD method, with titanium tetraisopropoxide

\* Corresponding author. Tel.: +82 2 958 5688; fax: +82 2 958 6711.

\*\* Corresponding author at: Graduate School of Energy and Environmental System Engineering, University of Seoul, Seoul 130-743, Republic of Korea. Tel.: +82 2 2210 5623; fax: +82 2 2244 2245.

E-mail addresses: [jongsoo@kist.kr](mailto:jongsoo@kist.kr) (J. Jurng), [catalica@uos.ac.kr](mailto:catalica@uos.ac.kr) (Y.-K. Park).

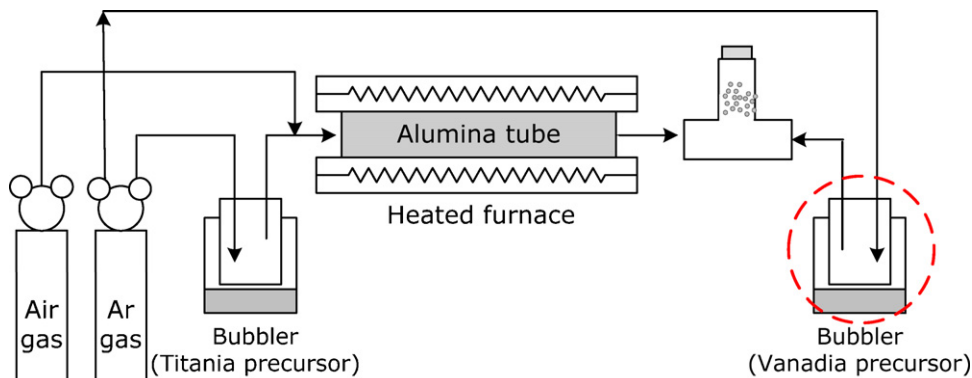


Fig. 1. A schematic diagram of the apparatus for modified-CVD.

$[(\text{CH}_3)_2\text{CHO}]_4\text{Ti}$ , TTIP, Aldrich, >97%) and vanadium oxytripropoxide ( $\text{VO}[\text{OCH}_2\text{CH}_2\text{CH}_2\text{CH}_3]_3$ , Aldrich, >98%) as the precursors. Fig. 1 shows a schematic diagram of the experimental apparatus, which consisted of two heated bubblers containing the precursors, a heated furnace and a T-junction connector. One bubbler was used for the conventional CVD process, whereas two bubblers were used for the modified CVD process.

To synthesize the  $\text{V}_2\text{O}_5/\text{TiO}_2$  nanocomposite particles, TTIP was introduced into the system through a bubbler using argon as the carrier gas. The TTIP precursor vapor was entrained by the carrier gas (argon) through the heated furnace and condensed into the  $\text{TiO}_2$  nanoparticles in the T-junction connector. The vanadium adhered to the  $\text{TiO}_2$  surface in the vapor phase.

The flow rates of air, as the dilute gas, and argon, as the carrier gas, for the generation of TTIP were fixed to 5.0 and 0.5 L/min, respectively. The flow rate of the carrier gas (argon) for the vanadium precursor was varied from 0.5 to 3.0 L/min to determine its effect on the vanadium concentration. The experiments were carried out in a furnace heated to 900 °C. The TTIP and vanadium precursor were vaporized in bubblers at 90 and 80 °C, respectively. Finally, the synthesized  $\text{V}_2\text{O}_5/\text{TiO}_2$  nanocomposite particles were calcined at 500 °C for 2 h in static air due to the anatase to rutile phase transformation above 550 °C. The nanocomposite particle samples were designated according to the expression, “flow rate of vanadium precursor  $\text{V}_2\text{O}_5/\text{TiO}_2$ ”. For example, the sample produced with a flow rate of the carrier gas for the vanadium precursor of 0.5 L/min was designated as 0.5  $\text{V}_2\text{O}_5/\text{TiO}_2$ .

The morphology and particle size were analyzed by transmission electron microscopy (TEM, Hitachi H-800) operated at an acceleration voltage of 200 kV. The surface layer composition of the particles was determined by X-ray photoelectron spectroscopy (XPS) using the Al K $\alpha$  line as the X-ray source. The Brunauer–Emmett–Teller (BET) measurements were also performed to obtain the specific surface area analysis of the nanocomposite particles. The mass ratio of  $\text{V}_2\text{O}_5$  and  $\text{TiO}_2$  was measured by inductively coupled plasma optical

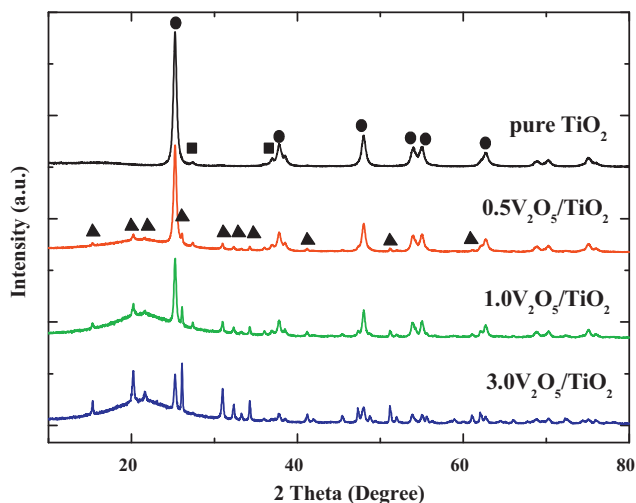


Fig. 2. XRD patterns of the pure  $\text{TiO}_2$ , 0.5  $\text{V}_2\text{O}_5/\text{TiO}_2$ , 1.0  $\text{V}_2\text{O}_5/\text{TiO}_2$  and 3.0  $\text{V}_2\text{O}_5/\text{TiO}_2$  (●: anatase, ■: rutile, and ▲:  $\text{V}_2\text{O}_5$ ).

Table 1  
Characteristics of the synthesized nanoparticles.

Sample	$S_{\text{BET}}$ ( $\text{m}^2 \text{g}^{-1}$ )	Particle size (nm)		Surface atomic concentration <sup>a</sup> (%)			$\text{V}_2\text{O}_5/\text{TiO}_2$ <sup>b</sup>
		XRD	TEM	O	Ti	V	
Pure $\text{TiO}_2$	78.47	11.5	11.5	64.87	35.13	0	0
0.5 $\text{V}_2\text{O}_5/\text{TiO}_2$	76.23	14.8	15.3	68.77	26.50	4.73	5.9
1.0 $\text{V}_2\text{O}_5/\text{TiO}_2$	72.20	33.5	33.2	67.03	17.67	15.30	8.3
3.0 $\text{V}_2\text{O}_5/\text{TiO}_2$	51.49	48.9	48.5	71.04	8.68	20.28	15.5

<sup>a</sup> XPS analysis.

<sup>b</sup> Mass ratio by ICP-OES.

emission spectrometry (ICP-OES). The X-ray diffraction (XRD) patterns of the nanocomposite particles were recorded on a DMAX-2500 (Rigaku Inc.; focal spot size: 5 mm<sup>2</sup>) diffractometer using a Cu rotating anode at a scan rate of

2 ° min<sup>-1</sup>. The surface morphology and elemental distribution of the V<sub>2</sub>O<sub>5</sub>/TiO<sub>2</sub> nanocomposite particles were examined by field emission scanning electron microscopy (SEM) and energy dispersive spectroscopy (EDS) (JSM-6700F, JEOL).

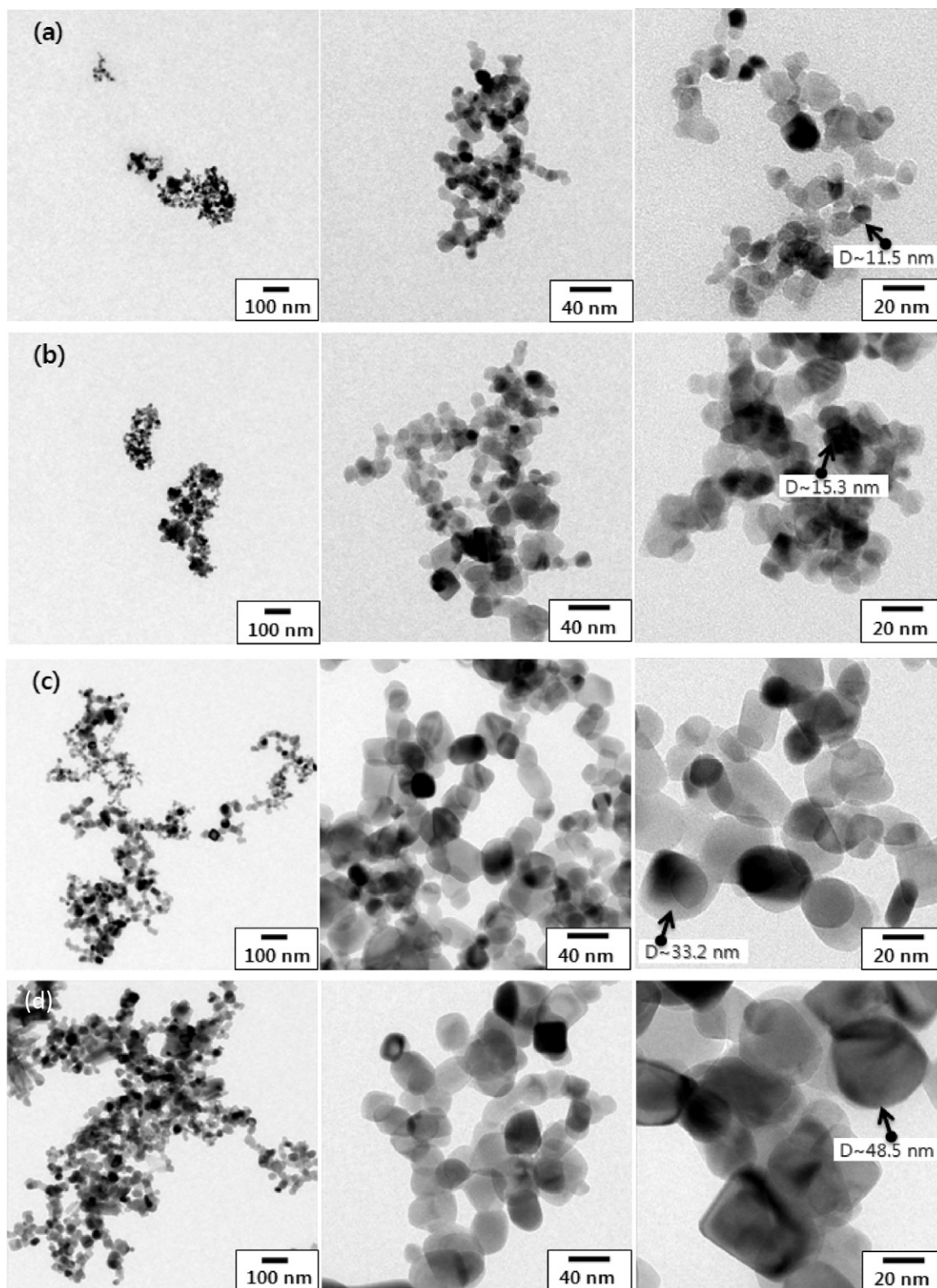


Fig. 3. TEM images of (a) pure TiO<sub>2</sub>, (b) 0.5 V<sub>2</sub>O<sub>5</sub>/TiO<sub>2</sub>, (c) 1.0 V<sub>2</sub>O<sub>5</sub>/TiO<sub>2</sub> and (d) 3.0 V<sub>2</sub>O<sub>5</sub>/TiO<sub>2</sub>.

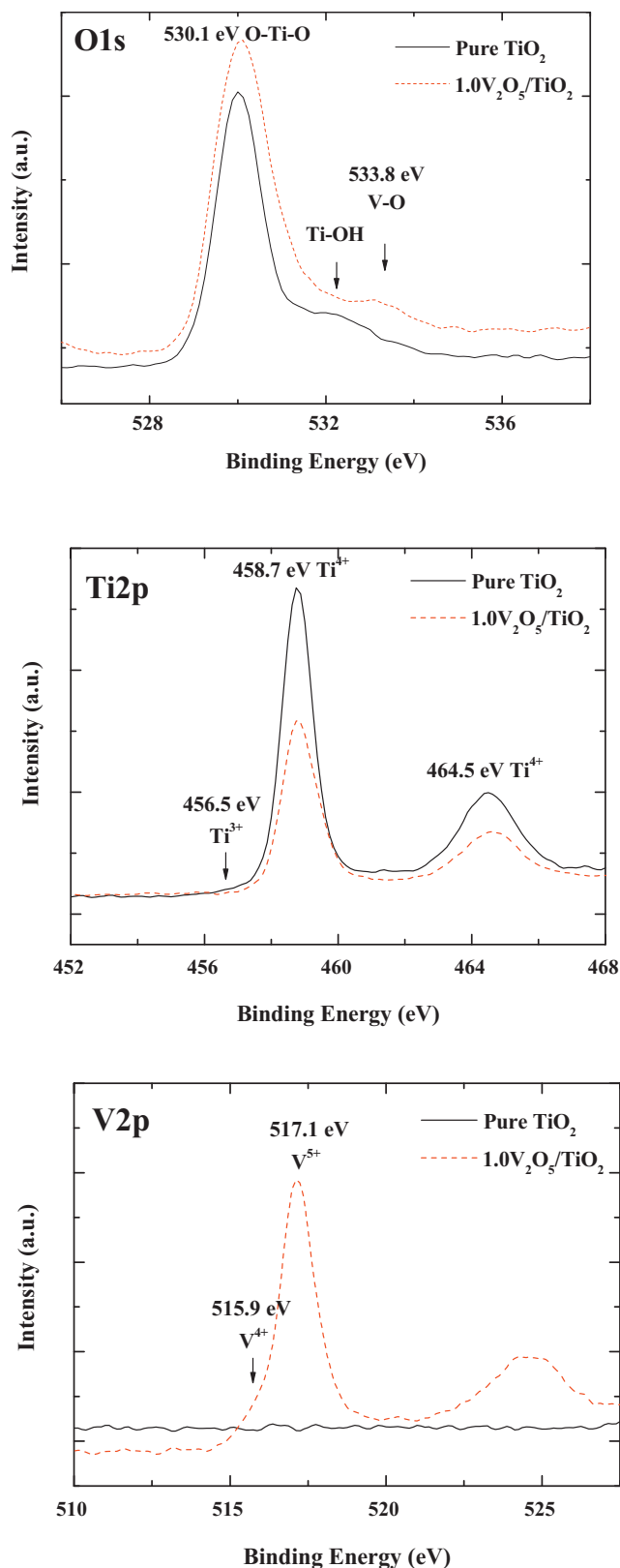


Fig. 4. The O1s, Ti2p and V2p high-resolved XPS spectra of the pure  $\text{TiO}_2$  and  $1.0 \text{ V}_2\text{O}_5/\text{TiO}_2$ .

### 3. Results and discussion

The properties of the  $\text{V}_2\text{O}_5/\text{TiO}_2$  nanocomposite particles were examined by varying the gas flow rate of the vanadium precursor with a fixed Ti precursor. Table 1 lists the specific surface area, particle size, surface atomic concentration and mass ratio of the  $\text{V}_2\text{O}_5/\text{TiO}_2$  nanocomposite particles. The flow rate of the vanadium precursor had a significant effect on the specific surface area, particle size and surface atomic concentration. The vanadium atomic concentration increased with increasing gas flow rate of the vanadium precursor. This can be explained by the titanium being formed as a particle, which was subsequently deposited with vanadium in the vapor state by the addition of vanadium to titanium in a one step simultaneous synthesis of  $\text{V}_2\text{O}_5/\text{TiO}_2$ . The specific surface areas of the pure  $\text{TiO}_2$ ,  $0.5 \text{ V}_2\text{O}_5/\text{TiO}_2$ ,  $1.0 \text{ V}_2\text{O}_5/\text{TiO}_2$  and  $3.0 \text{ V}_2\text{O}_5/\text{TiO}_2$  samples were 78.47, 76.23, 72.20 and  $51.49 \text{ m}^2 \text{ g}^{-1}$ , respectively, and the particle size of the nanoparticle increased from 11.5 to 48.9 nm. The BET data showed that the specific surface area of the  $\text{V}_2\text{O}_5/\text{TiO}_2$  nanocomposite particles was lower than that of pure  $\text{TiO}_2$ . In addition, XRD and TEM showed that an increase in flow rate of the vanadium precursor leads to an increase in primary particle size. In addition, the decrease in surface area is strongly related to the primary particle size, i.e. larger particles have a smaller surface area. The vanadium concentration and particle size increased with increasing gas flow rate of the vanadium precursor, which resulted in a decrease in specific surface area with increasing vanadium concentration [17] and particle size (Table 1).

$\text{TiO}_2$  anatase phase has a larger surface area and pore volume than the  $\text{TiO}_2$  rutile phase [18]. Fig. 2 shows the XRD patterns of the  $\text{V}_2\text{O}_5/\text{TiO}_2$  nanocomposite particles with different flow rates of the vanadium precursor. For pure  $\text{TiO}_2$  without  $\text{V}_2\text{O}_5$ , strong diffraction peaks for anatase were observed along with very weak peaks for rutile. XRD indicated a predominance of  $\text{TiO}_2$  anatase in all samples. When the vanadium precursor was introduced to the system, peaks associated with a  $\text{V}_2\text{O}_5$

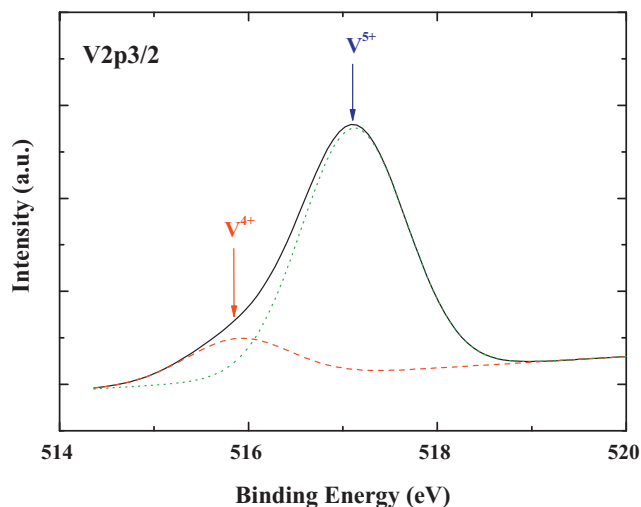
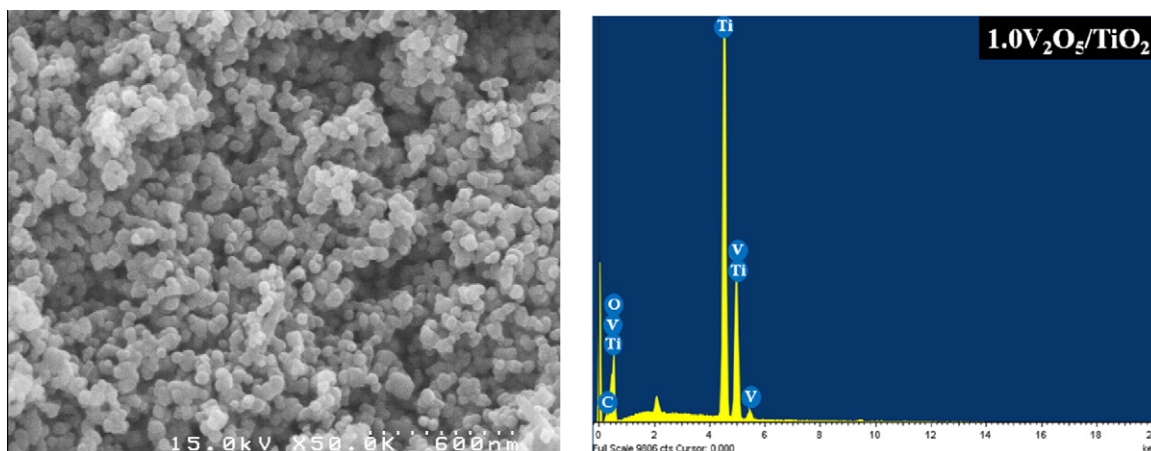


Fig. 5. Curve fitting of the V2p XPS spectra of  $1.0 \text{ V}_2\text{O}_5/\text{TiO}_2$ .

Fig. 6. SEM-EDS images of 1.0  $V_2O_5/TiO_2$ .

crystalline phase were observed in all samples. The intensity of the anatase peaks decreased with increasing V precursor vapor. The amorphous component increased with increasing V precursor vapor, which might explain the decrease in the anatase peak. XRD confirmed the existence of  $V_2O_5$  and  $TiO_2$  in the composite, highlighting the successful introduction of  $V_2O_5$  onto  $TiO_2$ .

Fig. 3 shows TEM images of the pure  $TiO_2$ , 0.5  $V_2O_5/TiO_2$ , 1.0  $V_2O_5/TiO_2$  and 3.0  $V_2O_5/TiO_2$  samples synthesized using the modified-CVD process. All samples obtained in the experiments had almost polyhedral structures. The particle size and degree of aggregation increased significantly with increasing flow rate of the vanadium precursor. The pure  $TiO_2$  particles (Fig. 3a) had a rare polyhedral structure with a diameter  $<20$  nm. In contrast, the diameter of the  $V_2O_5/TiO_2$  nanocomposite particles synthesized using the modified-CVD process was  $>20$  nm, and the structure was a dense polyhedral [19]. Particle sizes obtained from the TEM images and XRD line broadening were almost consistent. The increased particle size might be due to the formation of agglomerates with increasing vanadium precursor flow rate [20].

The surface of the synthesized  $V_2O_5/TiO_2$  nanocomposite particles was examined by XPS. Fig. 4 shows the highly resolved O1s, Ti2p and V2p core-level spectra of the pure  $TiO_2$  and 1.0  $V_2O_5/TiO_2$ . The O1s peak was fitted to Gaussian peaks at 530.1 eV, which arose from the lattice oxygen (O–Ti–O) and surface hydroxyl groups (Ti–OH) of pure  $TiO_2$ , whereas a peak for V–O was observed at 533.8 eV. The two peaks in the Ti2p XPS spectrum at 458.7 and 464.5 eV were assigned to Ti2p<sub>1/2</sub> and 2p<sub>3/2</sub>, respectively. The shapes of the peaks were symmetrical, indicating that  $Ti^{4+}$  was present as mainly pure  $TiO_2$ , whereas the Ti2p peak became wide and unsymmetrical after the simultaneous synthesis of 1.0  $V_2O_5/TiO_2$ . The 1.0  $V_2O_5/TiO_2$  nanocomposite particles consisted of two chemical states,  $V^{4+}$  and  $V^{5+}$ , for which the peaks were observed at 515.9 and 517.1 eV, respectively. The high-resolution XPS spectra of V2p<sub>3/2</sub> were investigated by Gaussian–Lorentzian curve fitting. As shown in Fig. 5, the peak at 515.9 eV indicates the presence of a  $V^{4+}$  valance state, whereas the peak at a higher BE of 517.1 eV corresponded to the higher oxidation state of

vanadium, i.e.  $V^{5+}$ . Therefore, the XPS results carried out on the sample surface showed that only  $V^{4+}$  and  $V^{5+}$  oxidation states of vanadium were present [21–24]. This is a very important point because control of the concentration of  $V_2O_5$  adhered to  $TiO_2$  is crucial for the catalytic properties of the material.

Fig. 6 shows SEM-EDS images of the 1.0  $V_2O_5/TiO_2$  nanocomposite particles prepared using the modified-CVD method. The prepared particles were almost spherical in shape and showed a morphology consisting of agglomerated particles. EDS demonstrated Ti, V and O on the  $V_2O_5/TiO_2$  surface. The results obtained from SEM-EDS clearly demonstrated that the synthesized  $V_2O_5/TiO_2$  consisted of nanocomposite particles.

#### 4. Conclusions

$V_2O_5/TiO_2$  nanocomposite particles were synthesized using a modified-CVD process employing two metal-organic precursors.  $V_2O_5/TiO_2$  nanocomposite particles with various vanadium concentrations and characteristics were obtained by controlling the flow rate of the vanadium precursor. XPS confirmed that the nanocomposite particles consisted of Ti, V and O. The crystalline phases of the  $V_2O_5/TiO_2$  nanocomposite particles were  $TiO_2$  anatase, very weak  $TiO_2$  rutile and  $V_2O_5$  structure. The particle size and degree of aggregation increased significantly with increasing flow rate of the vanadium precursor. Since this method allows the simultaneous synthesis of  $V_2O_5/TiO_2$  nanocomposite particles, it is expected to have potential applications in a range of fields. Furthermore, this technique can be applied in areas, such as catalysts, photoelectron materials and sensors.

#### References

- [1] S. Albonetti, G. Baldi, A. Barzanti, A.L. Costa, J. Epoupa Mengou, F. Trifiro, A. Vaccari, Chlorinated organics total oxidation over  $V_2O_5/TiO_2$  catalysts prepared by polyol-mediated synthesis, *Appl. Catal., A* 325 (2007) 309–315.
- [2] G. Silversmit, H. Poelman, D. Depla, N. Barrett, G.B. Marin, R.D. Gryse, A fully oxidized  $V_2O_5/TiO_2(001)$ -anatase system studied with in situ synchrotron photoelectron spectroscopy, *Surf. Sci.* 584 (2005) 179–186.



- [3] X. Liang, T. Zhong, B.F. Quan, B. Wang, H.S. Guan, Solid-state potentiometric  $\text{SO}_2$  sensor combining NASICON with  $\text{V}_2\text{O}_5$ -doped  $\text{TiO}_2$  electrode, *Sens. Actuators B* 134 (2008) 25–30.
- [4] J.W. Liu, Q. Sun, Y.C. Fu, J.Y. Shen, Preparation and characterization of mesoporous  $\text{VO}_x$ - $\text{TiO}_2$  complex oxides for the selective oxidation of methanol to dimethoxymethane, *J. Colloid Interface Sci.* 335 (2009) 216–221.
- [5] P. Courtine, E. Bordes, Mode of arrangement of components in mixed vanadia catalyst and its bearing for oxidation catalysis, *Appl. Catal., A* 157 (1997) 45–65.
- [6] I.E. Wachs, B.M. Weckhuysen, Structure and reactivity of surface vanadium oxide species on oxide supports, *Appl. Catal., A* 157 (1997) 67–90.
- [7] G.C. Bond, Preparation and properties of vanadia/titania monolayer catalysts, *Appl. Catal., A* 157 (1997) 91–103.
- [8] J.G. Yu, J.F. Xiong, B. Cheng, S.W. Liu, Fabrication and characterization of Ag- $\text{TiO}_2$  multiphase nanocomposite thin films with enhanced photocatalytic activity, *Appl. Catal., B* 60 (2005) 211–221.
- [9] M.G. Bonne, S. Pronier, F. Can, X. Courtois, S. Valange, J.M. Tatibouet, S.B. Royer, P. Marecot, D. Duprez, Synthesis and characterization of high surface area  $\text{TiO}_2/\text{SiO}_2$  mesostructured nanocomposite, *Solid State Sci.* 12 (2010) 1002–1012.
- [10] R.T. Rajendra Kumar, B. Karunagaran, S. Venkatachalam, D. Mangalaraja, S.K. Narayandass, R. Kesavamoorthy, Influence of deposition temperature on the growth of vacuum evaporated  $\text{V}_2\text{O}_5$  thin films, *Mater. Lett.* 57 (2003) 3820–3825.
- [11] Z.F. Liu, J.W. Li, J. Ya, Y. Xin, Z.G. Jin, Mechanism and characteristics of porous ZnO films by sol-gel method with PEG template, *Mater. Lett.* 62 (2008) 1190–1193.
- [12] J. Klanwan, N. Akrapattangkul, V. Pavarajarn, T. Seto, Y. Otani, T. Charinpanitkul, Single-step synthesis of MWCNT/ZnO nanocomposite using co-chemical vapor deposition method, *Mater. Lett.* 64 (2010) 80–82.
- [13] J.F. Zhang, R. Tu, T. Goto, Preparation of carbon nanotube by rotary CVD on Ni nano-particle precipitated cBN using nickelocene as a precursor, *Mater. Lett.* 65 (2011) 367–370.
- [14] K. Nakasoa, K. Okuyamaa, M. Shimadaa, S.E. Pratsinisb, Effect of reaction temperature on CVD-made  $\text{TiO}_2$  primary particle diameter, *Chem. Eng. Sci.* 58 (2003) 3327–3335.
- [15] H. Xie, G. Gao, Z. Tian, N. Bing, L. Wang, Synthesis of  $\text{TiO}_2$  nanoparticles by propane/air turbulent flame CVD process, *Particuology* 7 (2009) 204–210.
- [16] E. Park, S. Chin, J. Kim, G.N. Bae, J. Jurng, Preparation of  $\text{MnO}_x/\text{TiO}_2$  ultrafine nanocomposite with large surface area and its enhanced toluene oxidation at low temperature, *Powder Technol.* 208 (2011) 740–743.
- [17] S. Karamat, R.S. Rawat, P. Lee, T.L. Tan, R.V. Ramanujan, W. Zhou, Structural, compositional and magnetic characterization of bulk  $\text{V}_2\text{O}_5$  doped ZnO system, *Appl. Surf. Sci.* 256 (2010) 2309–2314.
- [18] K.Y. Jung, Y.R. Jung, J.K. Jeon, J.H. Kim, Y.K. Park, S.D. Kim, Preparation of mesoporous  $\text{V}_2\text{O}_5/\text{TiO}_2$  via spray pyrolysis and its application to the catalytic conversion of 1,2-dichlorobenzene, *J. Ind. Eng. Chem.* 17 (2011) 144–148.
- [19] S.M. Chin, E.S. Park, M.S. Kim, J.S. Jurng, Photocatalytic degradation of methylene blue with  $\text{TiO}_2$  nanoparticles prepared by a thermal decomposition process, *Powder Technol.* 201 (2010) 171–176.
- [20] T. Mitsui, K. Tsutsui, T. Matsui, R. Kikuchi, K. Eguchi, Catalytic abatement of acetaldehyde over oxide-supported precious metal catalysts, *Appl. Catal., B* 78 (2008) 158–165.
- [21] D. Habel, J.B. Stelzer, E. Feike, C. Schröder, A. Hösch, C. Hess, A. Knop-Gericke, J. Caro, H. Schubert, Phase development in the catalytic system  $\text{V}_2\text{O}_5/\text{TiO}_2$  under oxidising conditions, *J. Eur. Ceram. Soc.* 26 (2006) 3287–3294.
- [22] B. Liua, X. Wang, G. Cai, L. Wen, Y. Song, X. Zhao, Low temperature fabrication of V-doped  $\text{TiO}_2$  nanoparticles, structure and photocatalytic studies, *J. Hazard. Mater.* 169 (2009) 1112–1118.
- [23] G. Silversmit, D. Depla, H. Poelman, G.B. Marin, R.D. Gryse, Determination of the V2p XPS binding energies for different vanadium oxidation states ( $\text{V}^{5+}$  to  $\text{V}^{0+}$ ), *J. Electron Spectrosc. Relat. Phenom.* 135 (2004) 167–175.
- [24] Z. Zhang, C. Shao, L. Zhang, X. Li, Y. Liu, Electrospun nanofibers of V-doped  $\text{TiO}_2$  with high photocatalytic activity, *J. Colloid Interface Sci.* 351 (2010) 57–62.